Hindawi Publishing Corporation
ISRN Civil Engineering
Volume 2013, Article ID 348973, 11 pages
http://dx.doi.org/10.1155/2013/348973

Research Article

3D FE Analysis of an Embankment Construction on GRSC and Proposal of a Design Method

Yogendra K. Tandel, Chandresh H. Solanki, and Atul K. Desai

Applied Mechanics Department, NIT Surat, Surat 395007, India

Correspondence should be addressed to Yogendra K. Tandel; tandel.yogendra@gmail.com

Received 30 November 2012; Accepted 7 February 2013

Academic Editors: N. D. Lagaros, H.-L. Luo, A. A. Torres-Acosta, and B. Uy

Stone column is often employed for strengthening of an embankment seated on deep soft clay. But in very soft clay having undrained shear strength less than or equal to 15 kPa, stone column may not derive adequate load carrying capacity and undergo large lateral deformation due to inadequate lateral confinement. In such circumstances, reinforcement to individual stone column by geosynthetics enhances load carrying capacity and reduces lateral deformation. This paper addresses parametric study on behaviour of embankment resting on Geosynthetic Reinforced Stone Column (GRSC) considering parameters such as stone column spacing to diameter ratio, deformation modulus of stone column material, geosynthetic stiffness, thickness of soft clay, and height of embankment by 3D numerical analysis. Finally, equation for Settlement Improvement Factor (SIF), defined as ratio between settlement of embankment without treatment and with geosynthetic reinforced stone column, is proposed that correlates with the major influence parameters such as stone column spacing to diameter ratio, deformation modulus of soft clay, and geosynthetic stiffness.

1. Introduction

Embankment seated on deep soft clay may undergo large settlement both vertically and horizontally. Various ground improvement techniques adopted to mitigate the settlements are stone column [1, 2], preconsolidation using prefabricated vertical drains [3, 4], vacuum preconsolidation [5, 6], deep mixed column [7, 8], and so forth. Provision of stone column in the embankment foundation has advantage of (1) reinforcing effect, (2) reduction in settlement, and (3) acceleration of consolidation settlement.

However, in soft clay having undrained cohesion less than or equal to 15 kPa, there will be excessive lateral deformation of stone column. Also, soft clay may penetrate into the stone column [9].

To overcome these problems, individual stone column may be reinforced peripherally by using a suitable geosynthetic. Numerous researchers have acknowledged this concept [10–18].

Most of the previous studies have focused on the effect of geosynthetic reinforcement on load carrying capacity of isolated stone column only. Very few authors have studied behaviour of GRSC under long-term loading condition, that is, embankment loading [19–21].

Current study examines the performance of embankment supported on GRSC. Effect of GRSC spacing to diameter ratio, deformation of stone column material, geosynthetic stiffness, thickness of soft clay, and height of embankment on embankment settlement is studied. Based on the present study, equation for SIF is proposed.

2. Parametric Studies

A hypothetical embankment construction on GRSC is considered. For the parametric study, one parameter was varied at a time while keeping other parameters constant. A detail of embankment geometry along with GRSC-reinforced ground is discussed in the following sections.

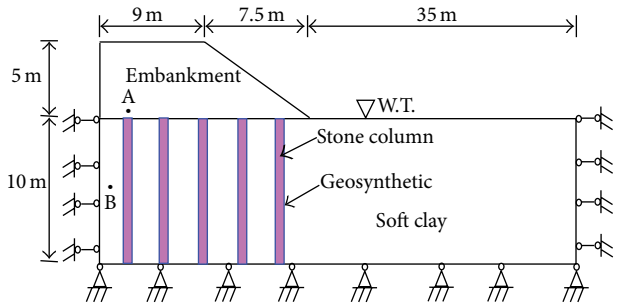

Figure 1: Schematic diagram of embankment supported on GRSC.

Table 1: Parameters varied.

Parameter	Range
Spacing of GRSC: S (m)	1.5, 2.0, 2.5*, 3.0
Deformation modulus of stone column material: E_{sc} (kpa)	30000, 35000*, 40000, 45000, 50000
Deformation modulus of embankment fill: E_{fill} (kpa)	30000*, 35000, 40000
Height of an embankment: h (m)	5*, 7.5, 10
Thickness of soft clay: H (m)	5, 10*, 15
Geosynthetic stiffness: J (kN/m)	500, 1000*, 2000, 4000, 8000

*Parameter for bench mark case.

2.1. Description GRSC-Reinforced Ground and Embankment. Embankment geometry and GRSC-reinforced ground for bench mark case are schematically shown in Figure 1. Due to symmetry, only half of the embankment was modeled to save computation time. As seen in this figure, a 33 m wide embankment having side slope 1 V : 1.5 H is constructed on 10 m soft clay underlying by rigid layer. Diameter of stone column for all analysis was kept 0.80 m. The boundary effect was investigated to extend the right boundary successively up to 35 m from the toe of the embankment. It was found that it would be sufficient to eliminate the boundary effect if the boundary was set at 35 m from the toe.

In the analysis, spacing of GRSC (S), deformation modulus of stone column material (E_{sc}), deformation modulus of embankment fill (E_{fill}), height of an embankment (h), thickness of soft clay (H), and stiffness of geosynthetic stiffness (J) are varied, as summarized in Table 1. Parameters for the bench mark case are mentioned in Table 2. The properties of stone columns, soft soil, and embankment fill were selected in the middle of their typical ranges to leave enough margins for the variations in the parametric study. Geosynthetic stiffness "J" is the secant stiffness of the geosynthetic, which is defined as the ratio of tensile force per unit width to the average strain in the geosynthetic. The creep effects of the geosynthetic are not considered in this study, by assuming that the hoop tension force developed in the encasement is much smaller than the tensile capacity of the geosynthetic. The variation ranges of the geosynthetic stiffness were considered covering the typical ranges of the values in most actual projects.

The zone of interface between stone column-geosynthetic and geosynthetic-clay is a zone with very high difference in magnitudes in young's modulus of the order of ten times or more. Also, the shear strength properties of this zone depend on the method of installation of stone column. The previous two properties of the interface are very difficult to quantify, and also during the loading stages the stone column undergoes bulging and induces lateral displacement of clay in the radial direction, where the shearing phenomenon along the interface is nearly absent. Hence, to make the analysis simple, the interface element is not considered in the analysis [20].

3. FE Modeling

Full 3D model was developed to understand the long-term behaviour of GRSC-reinforced ground. The commercial FE package PLAXIS 3D [22] was used for the FE modelling. Typical full 3D model is shown in Figure 2. The model shown in Figure 2 consists of 45,066 nodes and 55,447 elements. Relatively fine mesh arrangements were used to allow for the use of small time step (i.e., 0.001 day onwards) to achieve greater accuracy in the beginning of consolidation process. The mesh was refined in the region of the column-soil interface to increase the accuracy of the predictions. The critical time step is calculated based on the material properties and geometry of the model based on the criterion given by PLAXIS and used in the analysis.

As displacement boundary is concerns, no displacements in the directions perpendicular to the symmetry planes and to the base were allowed. For the hydraulic boundary condition, the phreatic level was set at the top surface of the soft clay layer to generate a hydrostatic pore water pressure profile in the domain. A zero pore pressure boundary condition was applied at the top. The left boundary was assumed impervious to consider the fact that no flow entered or left the symmetry plane. Since the right boundary was too far from the embankment to have significant influence on the results, it was set impervious. The finite element mesh was developed using 10 node tetrahedral elements to represent soft clay, stone column, and embankment fill. The geosynthetic reinforcement was modeled as geogrid element available in PLAXIS 3D, composed of 6 node triangular surface elements. Finer mesh arrangements were used for all the analysis to achieve greater accuracy in the beginning of consolidation process. Mohr-coulomb failure criterion was adopted for stone columns, embankment fill, and soft clay having linearly elastic perfectly plastic behaviour. The geosynthetic was modeled as geogrid element available in PLAXIS 3D having axial stiffness only. After generation of initial stress and pore water pressure, stone column was model by replacing soft soil element by stone column, and the geosynthetic reinforcement was added as wished in place. The embankment was constructed in 1 m increment. Each layer of an embankment is constructed in 30 days and consolidated for further 30 days before application of the following stage. Afterwards, calculation was continued till excess pore water pressure reached near 1 kPa.

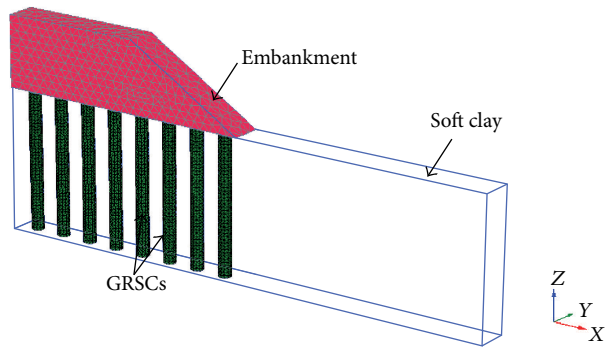

Figure 2: Full 3D model of embankment supported on GRSC.

Table 2: Parameters for the benchmark case.

Properties	Soft clay	Stone column	Embankment fill
Unsaturated unit weight (kN/m^3)	15	19	18
Saturated unit weight (kN/m^3)	17	20	20
Deformation modulus (kPa)	1000	35000	30000
Poisson ratio	0.35	0.3	0.3
Drained cohesion (kPa)	5	1	1
Drained friction angle (deg)	20	35	30
Dilation angle (deg)	0	5	0
Permeability (m/s)	1.0×10^{-9}	1.2×10^{-4}	1.2×10^{-5}

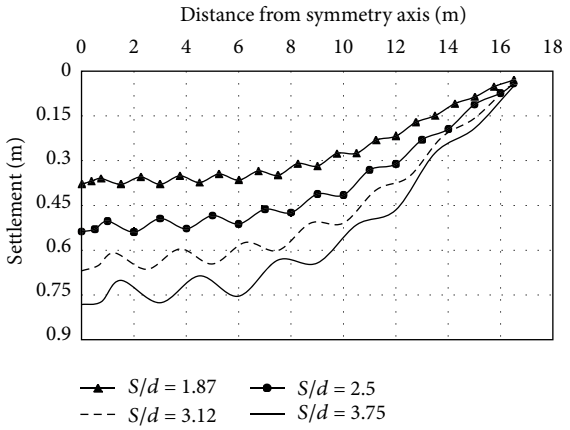

Figure 3: Settlement of natural ground surface for different S/d ratio.

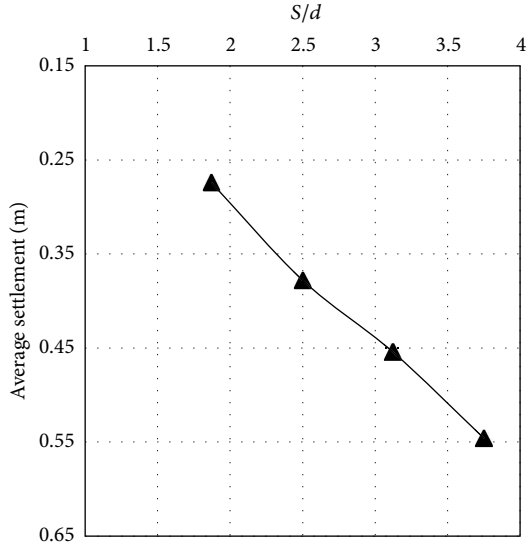

Figure 4: Average settlement for different S/d ratio.

4. Results and Discussion

In this section, influence of parameters, namely, S/d, E_{sc}, E_{fill}, J, h, and H on settlement of natural ground surface, average settlement of natural ground surface, and SIF is discussed. In addition, effect of S/d and geosynthetic stiffness on degree of consolidation, excess pore pressure, hoop forces in geosynthetic, and horizontal deformation of stone column is also discussed. In this study, degree of consolidation and excess pore pressure were observed for reference points A and B, respectively, as shown in Figure 1. Horizontal deformation and hoop force were computed for the extreme left stone column.

4.1. Influence of Spacing to Diameter Ratio of GRSC. Figure 3 shows the effect of spacing to diameter ratio of GRSC on settlement of natural ground surface at the end of consolidation. Settlement was computed for spacings 1.5 m, 2 m, 2.5 m and 3 m giving S/d ratio 1.87, 2.50, 3.12, and 3.75, respectively.

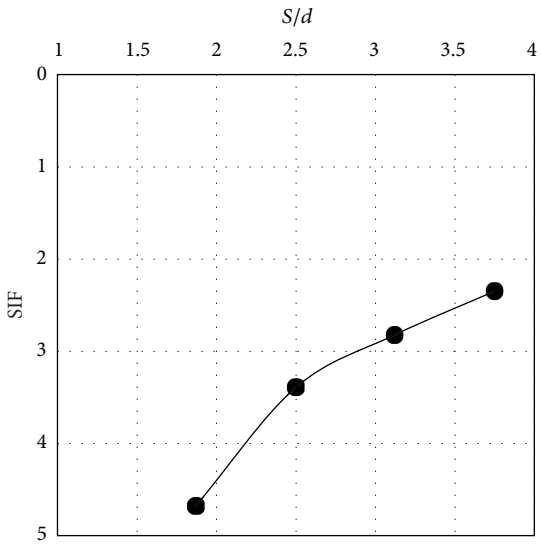

Figure 5: SIF for different S/d ratio.

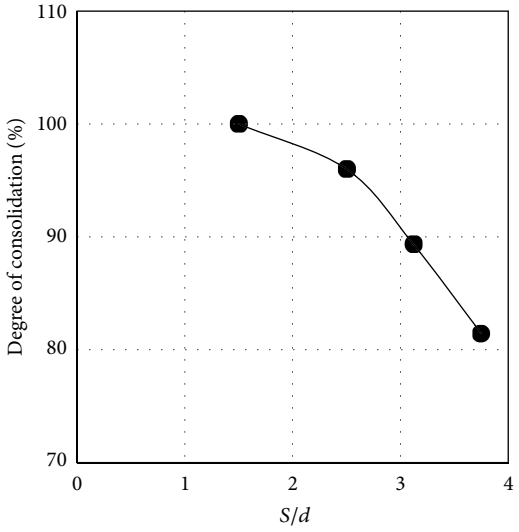

Figure 6: Effect of S/d ratio on degree of consolidation.

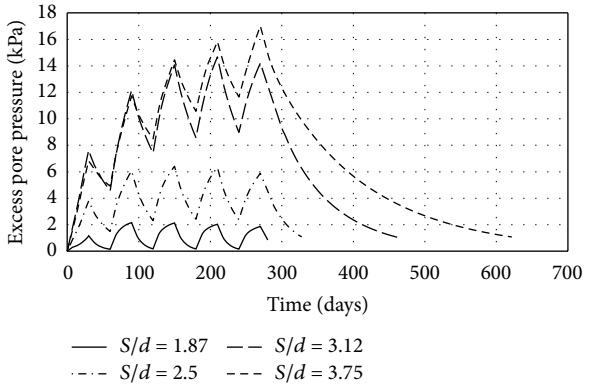

Figure 7: Effect of S/d ratio on excess pore pressure developed in clay.

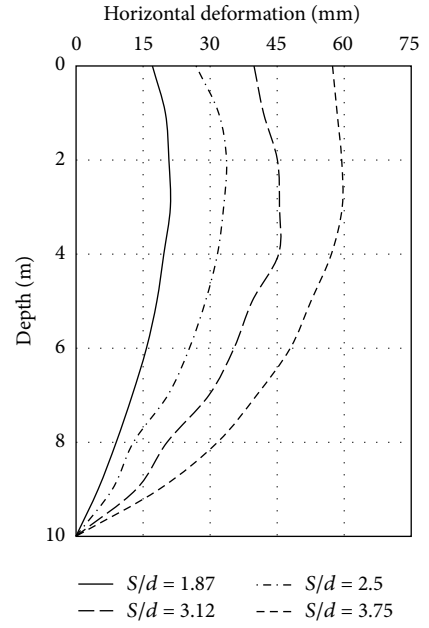

Figure 8: Effect of S/d ratio on horizontal deformation of stone column.

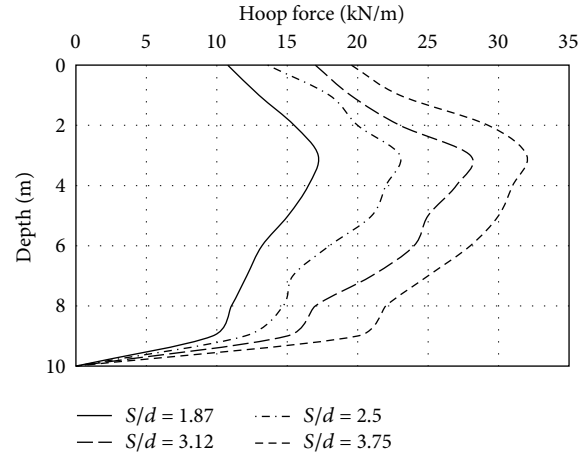

Figure 9: Effect of S/d ratio on hoop force developed in geosynthetic.

From this figure, it is clearly seen that S/d ratio has great effect on settlement of the natural ground surface.

Average settlement and SIF for different S/d ratios are shown in Figures 4 and 5, respectively. From Figure 4, it is observed that as S/d ratio decreases from 3.75 to 2.50, about 45% reduction in average settlement occurred. Figure 5 clearly indicates that SIF significantly increases with decreasing S/d ratio.

Since stone column also act as drain, decreasing S/d ratio increases the degree of consolidation. This is shown in Figure 6, where the degree of consolidation at 300 days is plotted for different S/d ratio. It is shown that larger S/d ratio yielded lower degree of consolidation. This is because of lower load transfer to the columns. Variation of excess pore pressure with time is plotted in Figure 7 for various S/d ratios. As

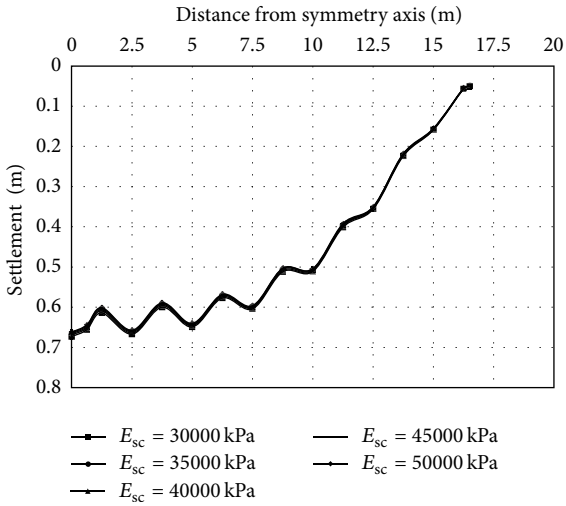

Figure 10: Settlement of natural ground surface for different deformation modulus of stone column material.

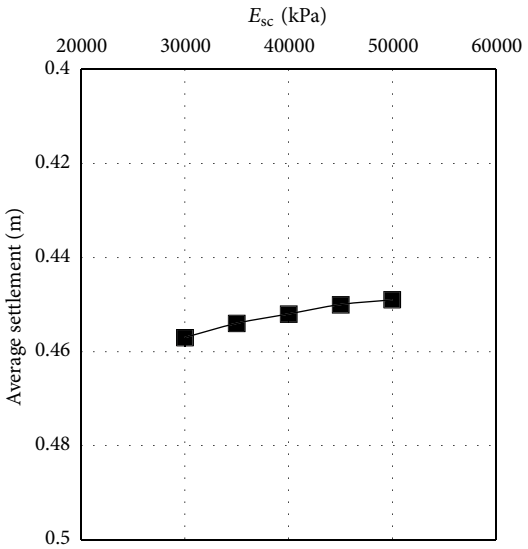

Figure 11: Average settlement for different deformation modulus of stone column material.

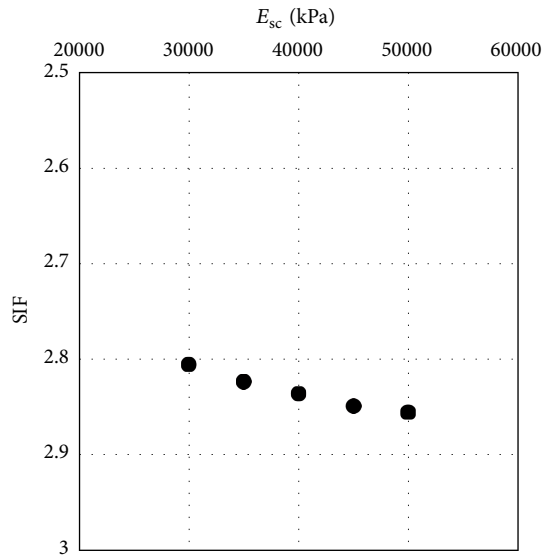

Figure 12: SIF for different deformation modulus of stone column material.

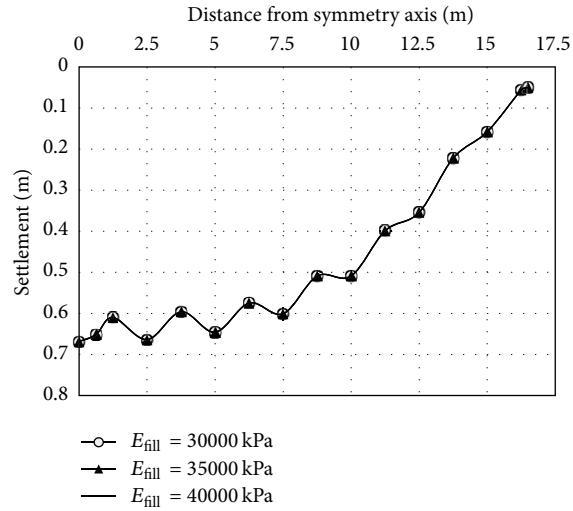

Figure 13: Settlement of natural ground surface for different deformation modulus of embankment fills.

shown in this figure, it can be seen that excess pore pressure increases with increasing S/d.

Horizontal deformation of the stone column and developed geosynthetic hoop force are illustrated in Figures 8 and 9, respectively, for different values of S/d. In Figure 8, it can be seen that horizontal deformation of the stone column tends to decrease sharply with decreasing S/d ratio. The maximum horizontal deformation was observed at a depth of 3 m, that is, 3.75 times the diameter of stone column from the top of the stone column. The geosynthetic hoop force profile, shown in Figure 9, tends to follow the general trend observed in the horizontal deformation profile with a tendency of increasing hoop force with increasing S/d ratio, showing a maximum hoop force of 32 kN/m occurring at 3.75 times the diameter of stone column below the top of the stone column for $S/d = 3.75$.

4.2. Influence of Deformation Modulus of Stone Column Material. The effect of deformation modulus of stone column material on natural ground surface settlement was studied by varying the modulus of column material from 30000 to 50000 kPa. Figures 10, 11, and 12 plot the natural ground surface settlement, average settlement, and SIF, respectively, for different values of column material modulus. Within the variation range of column modulus from 30,000 to 50,000 kPa, average settlement reduces about 8 mm only. This is because due to the geosynthetic reinforcement, columns were stiff enough as compared to surrounding soft clay due to which stable soil arching was formed.

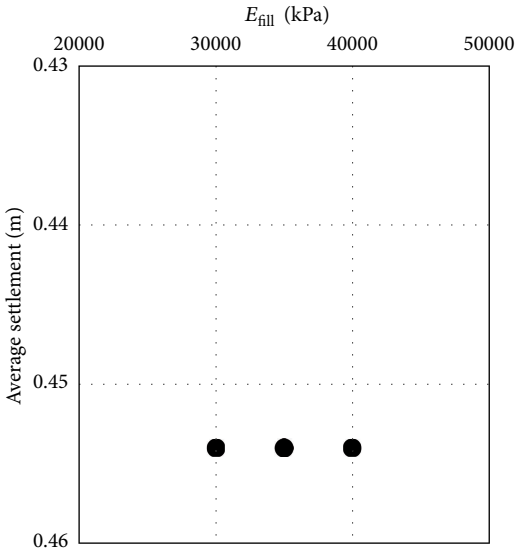

Figure 14: Average settlement for different deformation modulus of embankment fills.

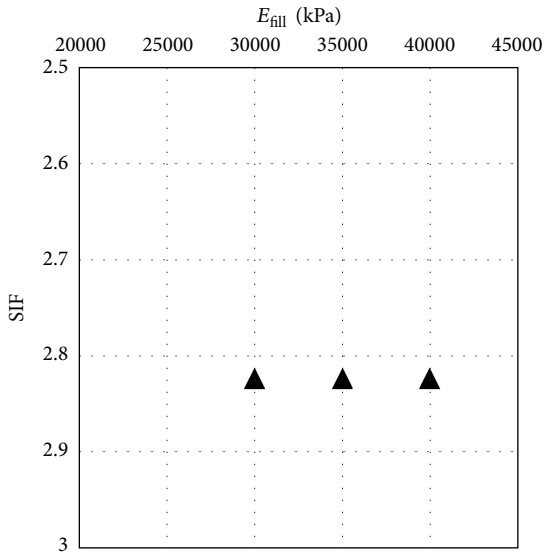

Figure 15: SIF for different deformation modulus of embankment fills.

4.3. Influence of Deformation Modulus of Embankment Fills. Settlement of natural ground surface, average settlement, and settlement improvement factor for different values of deformation modulus of embankment fill are illustrated in Figures 13, 14, and 15, respectively. As expected, embankment fill deformation modulus has no significant influence on natural ground surface settlement.

4.4. Influence of Geosynthetic Stiffness. In this section, influence of geosynthetic stiffness on settlement improvement factor is studied for a wide range of stiffness from 500 to 8000 kN/m. A nondimensional parameter (t) relating to

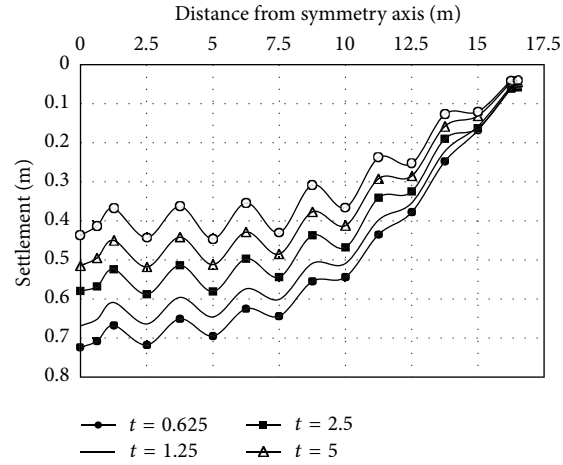

Figure 16: Settlement of natural ground surface for different t.

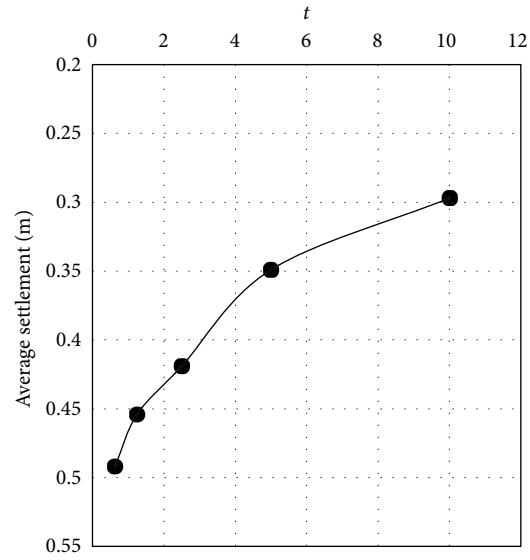

Figure 17: Average settlement for different t.

geosynthetic stiffness, soft clay deformation modulus, and diameter of GRSC is introduced as defined by (1).

For computing value of t, bench mark case stone column diameter and soil deformation modulus were used. Typical values of t for geosynthetic stiffness 500, 1000, 2000, 4000, and 8000 kN/m are 0.625, 1.25, 5, and 10, respectively. Consider

$$t = \frac{J}{d \cdot E_c}. \tag{1}$$

Settlement on the natural ground surface for different value of t is shown in Figure 16. This figure clearly indicates that increasing geosynthetic stiffness imparts higher confining pressure which leads to lower settlement. Average settlement and SIF for different geosynthetic stiffness are plotted in Figures 17 and 18, respectively. Figure 18 reveals that geosynthetic stiffness has great influence on SIF.

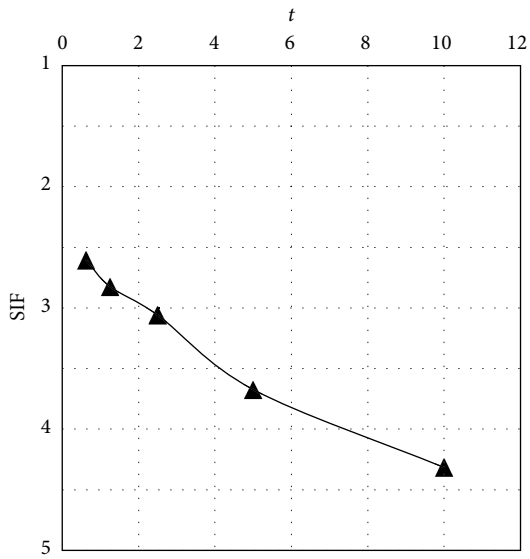

Figure 18: SIF for different t.

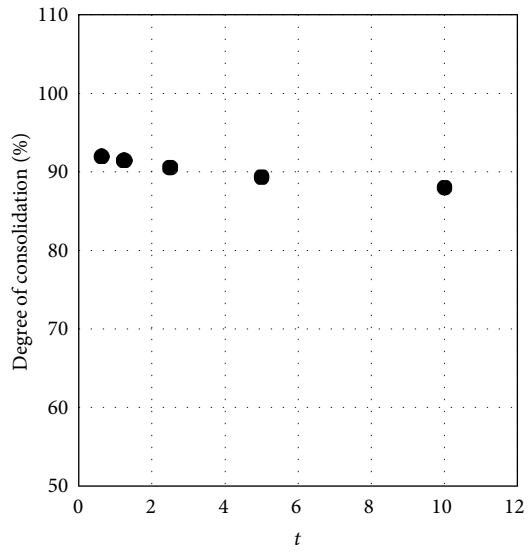

Figure 19: Effect of geosynthetic stiffness on degree of consolidation.

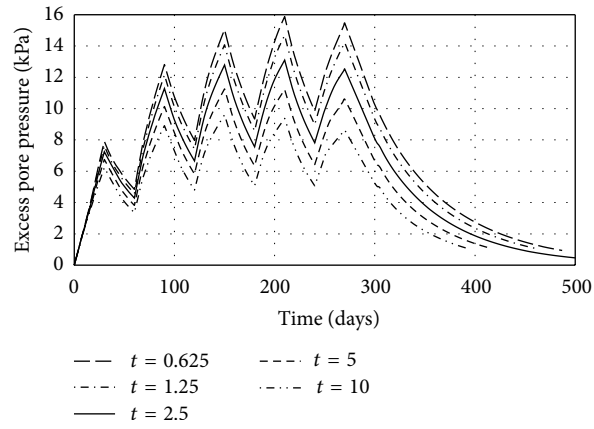

Figure 20: Effect of geosynthetic stiffness on excess pore pressure developed in clay.

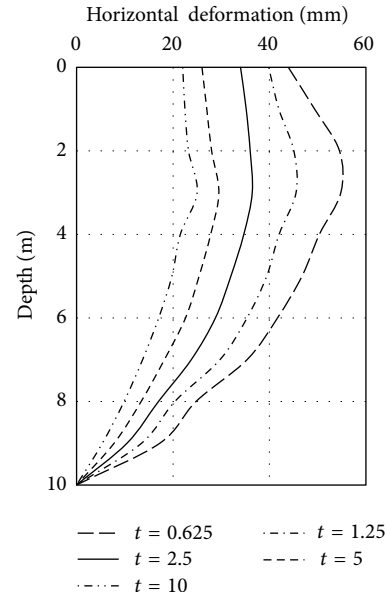

Figure 21: Effect of geosynthetic stiffness on horizontal deformation of stone column.

Variation of degree of consolidation at 300 days is seen in Figure 19. It is expected that the influence of geosynthetic stiffness on degree of consolidation is negligible. The progressive development of excess pore pressure with time is shown in Figure 20 for different geosynthetic stiffness. From this figure, it is clear that with increasing J, excess pore pressure decreases. This happens due to reduced embankment load transfer to the soft clay when adopting stiffer geosynthetic for reinforcement.

Horizontal deformation along the length of stone column is shown in Figure 21. As expected, horizontal deformation significantly reduces with increasing geosynthetic stiffness. The hoop tension forces developed in the geosynthetic are shown in Figure 22. The forces are high within depth equal to 3.75 times the diameter of stone column and remain more or less constant below this depth. The variation of these forcess follow the same trend as the horizontal deformation undergone by stone column.

4.5. Influence of Height of Embankment. The effect of embankment height on settlement was investigated herein for three different heights 5 m, 7.5 m, and 10 m. As expected, embankment height has remarkable effect on settlement as observed in Figures 23 and 24. As embankment height increases from 5 m to 7.5 m, average settlement increases by 45%. However, settlement improvement factor does not change significantly as predicted from Figure 25.

4.6. Influence of Thickness of Soft Clay. In this section, influence of soft clay thickness on the SIF is discussed. Three

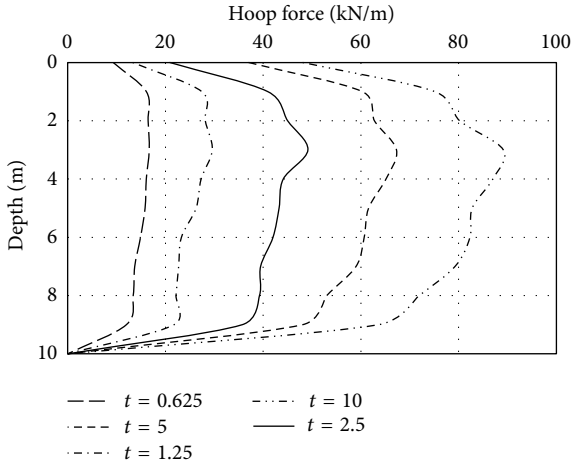

Figure 22: Effect of geosynthetic stiffness on hoop force developed in geosynthetic.

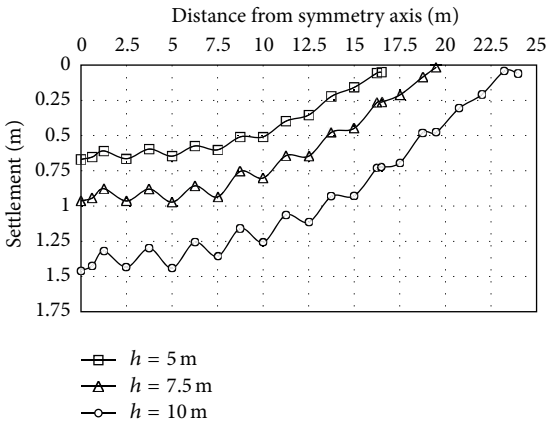

Figure 23: Settlement of natural ground surface for different height of embankment.

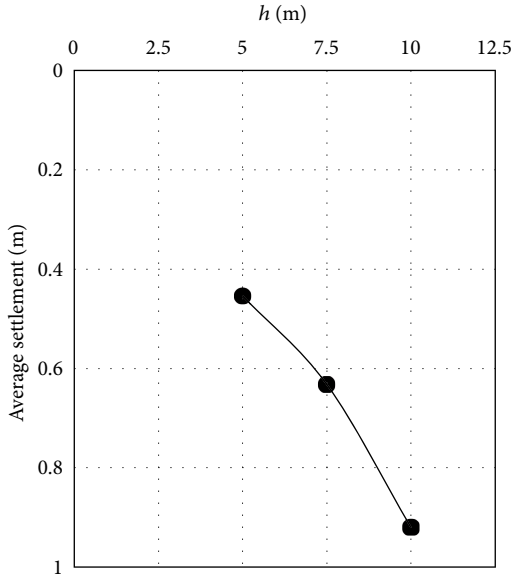

Figure 24: Average settlement for different height of embankment.

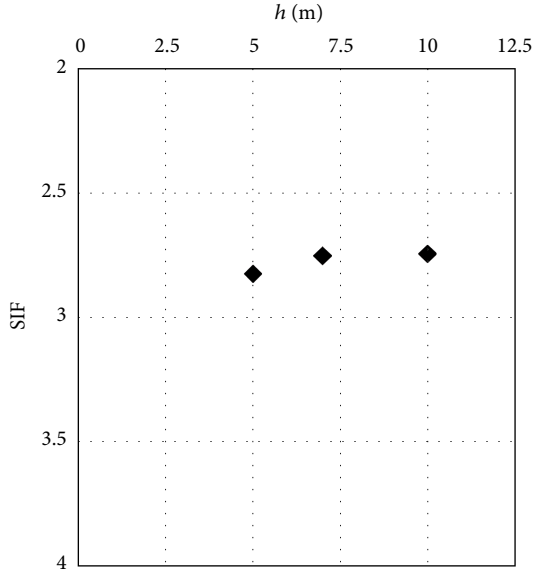

Figure 25: SIF for different height of embankment.

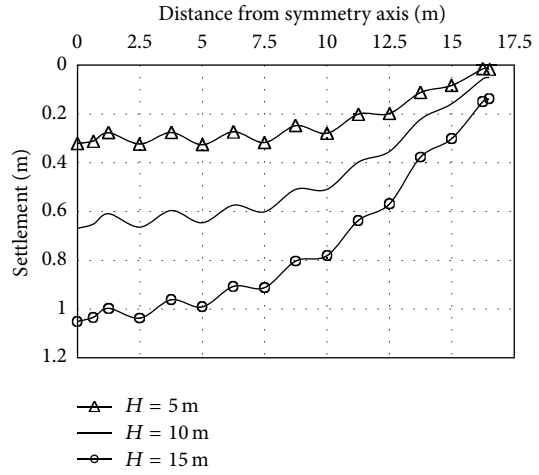

Figure 26: Settlement of natural ground surface for different thickness of soft clay.

soft clay thicknesses 5 m, 7.5 m, and 10 m are considered in the present study. The natural ground settlement at the end of consolidation period for various soft clay thicknesses is presented in Figure 26. Average settlement of ground surface and SIF for different soft clay thickness is shown in Figures 27 and 28, respectively. Figures 26 and 27 clearly show that increasing thickness of the soft clay increases settlement. However, the settlement improvement factor does not change significantly.

5. Proposal of Equation for SIF

Based on the present parametric study, it is revealed that only two parameters, namely, S/d and t, have significant influence on the SIF. So, herein, SIF equation is proposed for embankment construction of GRSC relating to the previous

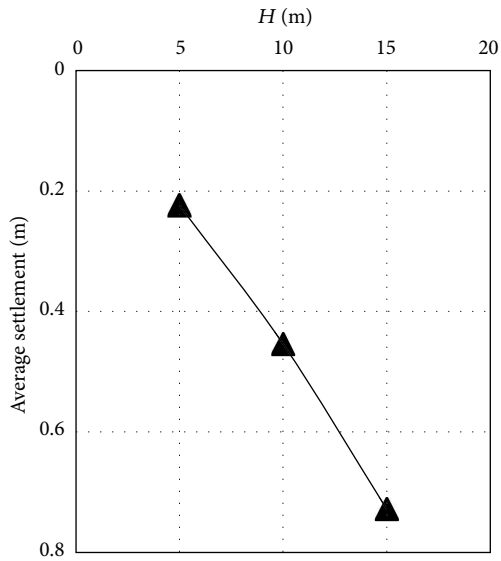

Figure 27: Average settlement for different thickness of soft clay.

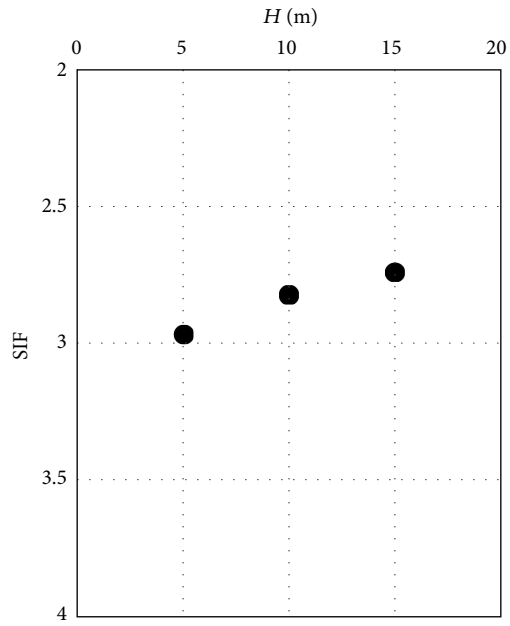

Figure 28: SIF for different thickness of soft clay.

two parameters. Relation between S/d, SIF, and t is plotted in Figure 29 and best fit equation is obtained as follows:

$$\text{SIF} = R1\left(\frac{S}{d}\right)^{R2}, \tag{2}$$

where $R1$ and $R2$ are factors that depend on t. Good correlation is obtained as values of R^2—the square of the Pearson product moment correlation coefficient—are always higher than 0.96.

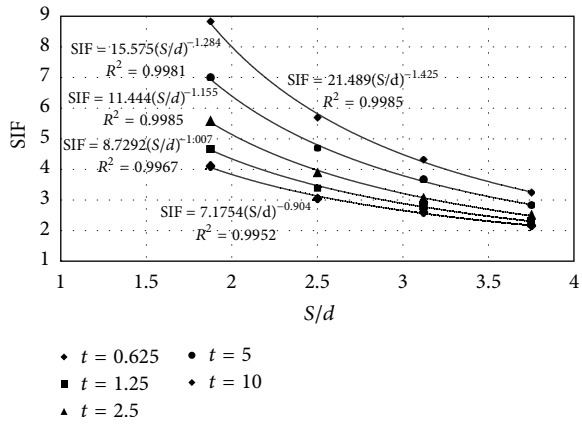

Figure 29: Correlation between SIF and S/d for different value of t.

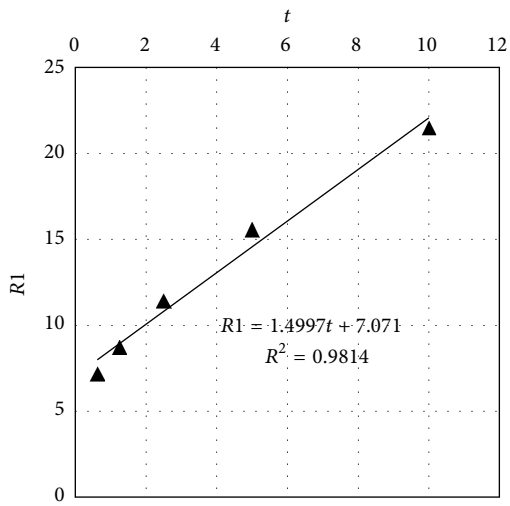

Figure 30: Correlation between $R1$ and t.

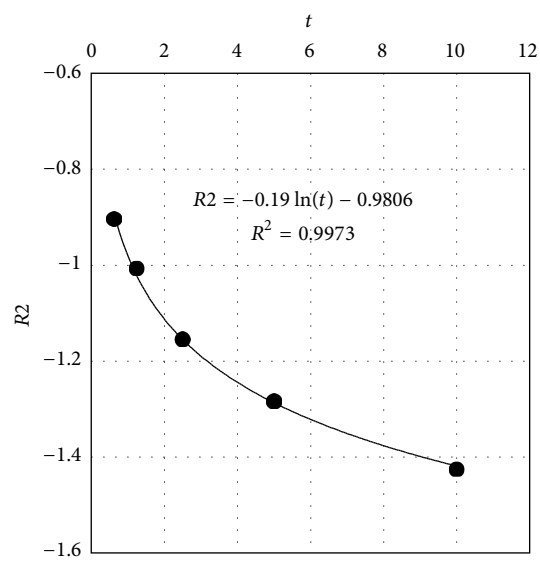

Figure 31: Correlation between $R2$ and t.

Table 3: Comparison of present results with existing projects.

Parameter	$S/d = 2.5$, $t = 1$		$S/d = 2.5$, $t = 4.67$		$S/d = 1.8$, $t = 1.04$	
	Project: Sinzhein 2000	Equation (4)	Project: DA-Erweiterung Hamburg 2002	Equation (4)	Project: Waltershof	Equation (4)
SIF	2.88	3.49	3.65	4.38	4.75	4.83

For generalisation of (2), correlation of factors $R1$ and $R2$ with t is mention in (3), obtained from Figures 30 and 31 respectively. Consider

$$R1 = 1.4997t + 7.071,$$
$$R2 = -0.19 \ln(t) - 0.9806. \quad (3)$$

Finally, substituting (3) in (2), the following design equation is obtained:

$$\text{SIF} = 1.4997t + 7.071\left(\frac{S}{d}\right)^{-0.19\ln(t)-0.9806}. \quad (4)$$

Results of SIF calculated from the proposed (4) are compared with the existing projects, namely, Sinzhein 2000, DA-Erweiterung Hamburg 2002 [23], and Waltershof 1996 [24]. The comparison is summarized in Table 3. The results of different projects are indicative purpose only, as different assumptions and parameters are considered in the present method.

6. Conclusions

Effect of stone column spacing to diameter ratio, deformation of stone column material and embankment fill, geosynthetic stiffness, height of embankment, and soft clay thickness on settlement of embankment was carried out by employing three-dimensional finite element modelling. The present study reveals that only two parameters, namely, stone column spacing to diameter ratio and non-dimensional parameter t (relating with geosynthetic stiffness, stone column diameter and soil modulus), have significant influence on the settlement improvement factor. Finally, equation for settlement improvement factor is proposed which relates with the previous two parameters. Additionally following overall conclusions can be drawn from the present study. (1) Horizontal deformation of stone column can be reduced by decreasing S/d ratio and/or increasing geosynthetic stiffness. (2) Hoop force is higher for low S/d ratio and higher geosynthetic stiffness. (3) Excess pore pressure reduces by increasing geosynthetic stiffness and/or reducing S/d ratios. (4) Degree of consolidation is increased with increasing S/d ratio but remains more or less constant for different geosynthetic stiffness.

Notations

GRSC: Geosynthetic Reinforced Stone Column
SIF: Settlement Improvement Factor
S: Spacing of stone column
d: Diameter of stone column
E_c: Deformation modulus of soft clay
E_{sc}: Deformation modulus of stone column material
E_{fill}: Deformation modulus of embankment fill
h: Height of an embankment
H: Thickness of soft clay
J: Tensile stiffness of geosynthetic material
t: Nondimensional parameter
$R1$, $R2$: Nondimensional factors.

Acknowledgment

The authors are thankful to the anonymous reviewers for their precise review and several suggestions for improving the presentation in the paper.

References

[1] D. Greenwood, "Mechanical improvement of soils below ground surface," in *Proceedings of Ground Engineering*, pp. 11–22, The Institution of Civil Engineers, London, UK, 1970.

[2] J. M. O. Hughes, N. J. Withers, and D. A. Greenwood, "Field trial of the reinforcing effect of a stone column in soil," *Geotechnique*, vol. 25, no. 1, pp. 31–44, 1975.

[3] A. T. Yeung, "Design curves for prefabricated vertical drains," *Journal of Geotechnical and Geoenvironmental Engineering*, vol. 123, no. 8, pp. 755–759, 1997.

[4] S. L. Shen, J. C. Chai, Z. S. Hong, and F. X. Cai, "Analysis of field performance of embankments on soft clay deposit with and without PVD-improvement," *Geotextiles and Geomembranes*, vol. 23, no. 6, pp. 463–485, 2005.

[5] J. Chu, S. W. Yan, and H. Yang, "Soil improvement by the vacuum preloading method for an oil storage station," *Geotechnique*, vol. 50, no. 6, pp. 625–632, 2000.

[6] B. Indraratna, C. Bamunawita, and H. Khabbaz, "Numerical modeling of vacuum preloading and field applications," *Canadian Geotechnical Journal*, vol. 41, no. 6, pp. 1098–1110, 2004.

[7] H. Krenn and M. Karstunen, "Numerical modelling of deep mixed columns below embankments constructed on soft soils," in *Proceedings of the 2nd International Workshop on Geotechnics of Soft Soils*, pp. 159–164, Glasgow, Scotland, September 2008.

[8] J. Huang and J. Han, "3D coupled mechanical and hydraulic modeling of a geosynthetic-reinforced deep mixed column-supported embankment," *Geotextiles and Geomembranes*, vol. 27, no. 4, pp. 272–280, 2009.

[9] D. Alexiew, D. Brokemper, and S. Lothspeich, "Geotextile Encased Columns (GEC): load capacity, geotextile selection and

pre-design graphs," in *Proceedings of the Geo-Frontiers*, pp. 497–510, ASCE Geotechnical Special Publication, Austin, Tex, USA, January 2005.

[10] S. Murugesan and K. Rajagopal, "Geosynthetic-encased stone columns: numerical evaluation," *Geotextiles and Geomembranes*, vol. 24, no. 6, pp. 349–358, 2006.

[11] M. Raithel and H. G. Kempfert, "Calculation models for dam foundations with geotextile-coated sand columns," in *Proceedings of the International Conference on Geotechnical and Geological Engineering (GeoEngg '00)*, p. 347, Melbourne, Australia, 2000.

[12] H. G. Kempfert, W. Möbius, P. Wallis, M. Raithel, M. Geduhn, and R. G. McClinton, "Reclaiming land with geotextile-encased columns," *Geotechnical Fabrics Report*, vol. 20, no. 6, pp. 34–39, 2002.

[13] M. Raithel, H. G. Kempfert, and A. Kirchner, "Geotextile Encased Columns (GEC) for foundation of a dike on very soft soils," in *Proceeding of 7th International Conference on Geosynthetics*, pp. 1025–1028, Balkema, The Netherlands, 2002.

[14] D. Brokemper, J. Sobolewski, D. Alexiew, and C. Brok, "Design and construction of geotextile encased columns supporting geogrid reinforced landscape embankments: Bastions Vijfwal Houten in the Netherlands," in *Proceeding of the 8th International Conference on Geosynthetics*, pp. 1681–1684, Amsterdam, The Netherlands, 2006.

[15] D. Lee, A. Song, S. Kim, and C. Yoo, "Short and long term load carrying capacity of geogrid-encased stone column-a numerical investigation," *Journal of Korean Geotechnical Society*, vol. 23, no. 8, pp. 5–16, 2007.

[16] C. Yoo, A. Song, S. Kim, and D. Lee, "Finite element modeling of geogrid-encased stone column in soft ground," *Journal of Korean Geotechnical Society*, vol. 23, no. 10, pp. 133–150, 2007.

[17] J. Gniel and A. Bouazza, "Improvement of soft soils using geogrid encased stone columns," *Geotextiles and Geomembranes*, vol. 27, no. 3, pp. 167–175, 2009.

[18] C. S. Wu and Y. S. Hong, "Laboratory tests on geosynthetic-encapsulated sand columns," *Geotextiles and Geomembranes*, vol. 27, no. 2, pp. 107–120, 2009.

[19] C. Yoo and S. B. Kim, "Numerical modeling of geosynthetic-encased stone column-reinforced ground," *Geosynthetics International*, vol. 16, no. 3, pp. 116–126, 2009.

[20] S. R. Lo, R. Zhang, and J. Mak, "Geosynthetic-encased stone columns in soft clay: a numerical study," *Geotextiles and Geomembranes*, vol. 28, no. 3, pp. 292–302, 2010.

[21] C. Yoo, "Performance of geosynthetic-encased stone columns in embankment construction: numerical investigation," *Journal of Geotechnical and Geoenvironmental Engineering*, vol. 136, no. 8, pp. 1148–1160, 2010.

[22] R. B. Brinkgreve and P. A. Vermeer, *PLAXIS 3D-Finite Element Code for Soil and Rocks Analysis*, Balkema, Rotterdam, The Netherlands, 2012.

[23] M. Raithel, A. Kirchner, C. Schade, and E. Leusink, "Foundation of constructions on very soft soils with geotextile encased columns—state of the art," in *Proceedings of the Geo-Frontiers*, pp. 1867–1877, Austin, Tex, USA, January 2005.

[24] H. G. Kempfert, "Embankment foundation on geotextile-coated sand columns in soft ground," in *Proceedings of the 1st Euopean Geosynthetics Conference in Maastrich, Geosynthetics. Applications, Design and Construction*, pp. 245–250, A. A. Balkema, Rotterdam, The Netherlands, 1996.